



Swansea University  
Prifysgol Abertawe



## Cronfa - Swansea University Open Access Repository

---

This is an author produced version of a paper published in :

*Corrosion*

Cronfa URL for this paper:

<http://cronfa.swan.ac.uk/Record/cronfa32003>

---

### Paper:

Fajardo, S., Glover, C., Williams, G. & Frankel, G. (2017). The Evolution of Anodic Hydrogen on High Purity Magnesium in Acidic Buffer Solution. *Corrosion*

<http://dx.doi.org/10.5006/2247>

---

This article is brought to you by Swansea University. Any person downloading material is agreeing to abide by the terms of the repository licence. Authors are personally responsible for adhering to publisher restrictions or conditions. When uploading content they are required to comply with their publisher agreement and the SHERPA RoMEO database to judge whether or not it is copyright safe to add this version of the paper to this repository.

<http://www.swansea.ac.uk/iss/researchsupport/cronfa-support/>

# The Evolution of Anodic Hydrogen on High Purity Magnesium in Acidic Buffer Solution

S. Fajardo<sup>a,b,\*</sup>, C.F. Glover<sup>c</sup>, G. Williams<sup>c</sup> and G.S. Frankel<sup>a</sup>

<sup>a</sup> Fontana Corrosion Center, Department of Materials Science and Engineering, The Ohio State University, Columbus, Ohio 43210, USA

<sup>b</sup> National Centre for Metallurgical Research (CENIM), Spanish Research Council (CSIC), Avda. Gregorio del Amo 8, Madrid 28040, Spain

<sup>c</sup> Materials Research Centre, College of Engineering, Swansea University, Bay Campus, Crymlyn Burrows, Swansea SA1 8EN, United Kingdom

## Abstract

Hydrogen evolution (HE) on anodically polarized Mg, commonly referred to as Negative Difference Effect, was studied by galvanodynamic measurements coupled with real-time gravimetric H<sub>2</sub> volume collection, the Scanning Vibrating Electrode Technique and potentiodynamic polarization experiments. High purity Mg (99.96% Mg) electrodes were studied in chloride-free 0.1 M citric acid solution buffered at pH with the aim of determining the source of anodic HE and the role of the corrosion film on the process. In such conditions of pH, the typical dark corrosion product exhibited in neutral and alkaline solutions was not found but the HE rate still increased with increasing potential. Evidence that HE on dissolving high purity Mg is associated with the regions dominated by the anodic dissolution reaction is provided. The role of noble impurity enrichment on the electrode surface during anodic polarization and the effect of Fe re-deposition are also discussed.

**Key Words:** hydrogen evolution; magnesium; scanning vibrating electrode technique; anodic polarization; NDE.

\*Corresponding Author: fajardo@cenim.csic.es, santiago.fajardo@gmail.com (S. Fajardo).

## 1. Introduction

Hydrogen evolution (HE) is the primary cathodic reaction on Mg surfaces under open circuit conditions due to their low corrosion potential [1]. However, under anodic polarization, enhanced rates of HE are exhibited as the extent of polarization increases [1-4] in contradiction with standard electrochemical kinetics theory. The persistent evolution of H<sub>2</sub> during anodic polarization of Mg remains a topic of intense research and, despite recent investigations that have apparently identified the primary source of HE [5], the cause of this phenomenon remains unproven. Other metals such as aluminum also exhibit this behavior [6-8].

The evolution of persistent anodic HE (also referred to as the negative difference effect, NDE) was investigated using an ultra-high purity (UHP) Mg specimen (nominal impurity content of about 1 ppmw) in NaCl solutions [5]. The scanning vibrating electrode technique (SVET), H<sub>2</sub> volume collection and electrochemical measurements provided evidence that the majority of the HE under anodic polarization originated from net anodic regions, in other words, from regions dominated by the anodic dissolution reaction. Even though the dark corrosion film that forms on corroding pure Mg surfaces exhibited enhanced catalytic activity towards the hydrogen evolution reaction (HER) compared with the un-attacked Mg surface, as observed by others [3, 9-13], it played a minor role in the HE at anodic potentials [5]. This contradicts explanations for anodic HE based on the role of the corrosion film [9, 12, 13].

The accumulation of impurities more noble than Mg on the electrode surface during polarization due to the preferential dissolution of the Mg matrix has also been

used to explain the enhanced rates of HE exhibited under anodic conditions [3, 14-17]. Even though the effect of noble impurities such as Fe on the corrosion behavior of pure Mg has been known for a long time [18], the idea that they could act as preferential cathodic sites for the HER on Mg during anodic polarization is rather recent. Taheri et al. [19] found small particles of Fe embedded in the dark corrosion film formed on corroding high purity Mg (HP, about 50 ppmw of Fe). However, it is not clear how a few Fe particles in a poorly conductive Mg oxide/hydroxide corrosion film could account for such large rates of anodic HE. Cain et al. found evidence of Fe enrichment in the residual oxide/hydroxide film or on the metal surface of an Mg anode using Rutherford Backscattering Spectrometry but reported the enrichment efficiency to be very poor [16]. Birbilis et al. [17] and Lysne et al. [14] confirmed this behavior with enrichment efficiencies lower than 1%. Another paper also concluded that noble impurity accumulation, studied by H<sub>2</sub> collection and electrochemical measurements had no impact on the high rates of HE on a HP Mg anode [3]. A recent study using an UHP Mg specimen (where the accumulation of impurities can be reasonably neglected) showed that the cathodic activation exhibited after anodic polarization is due to the enhanced catalytic activity towards the HER of the corrosion film formed during dissolution with respect to the uncorroded metal surface [5]. Fe re-deposition has also been proposed as a possible explanation for the occurrence of anodic HE [20]. Even though this mechanism may account for the increasing corrosion rates of Mg at open circuit conditions, its possible effect during anodic polarization remains unclear, as detailed elsewhere [5].

The aim of this paper, which was developed in parallel with another recent paper [5], is to further investigate the role of the film in the evolution of anodic H<sub>2</sub>. The effect of noble impurity accumulation on the electrode surface during dissolution and the re-

deposition of Fe are also discussed. Solid evidence that the evolution of hydrogen on anodically polarized Mg is primarily associated with the regions dominated by the anodic reaction is provided.

## 2. Experimental

HP Mg (with a nominal purity of about 99.96 %) was used as test specimen. This material was used in a previous study and its chemical composition is given elsewhere [3]. Samples were cold mounted in epoxy resin with a Cu wire attached to the rear part of the specimen to provide the electrical connection. Grinding to 1200 grit using silicon carbide papers under ethanol was carried out prior to testing. The electrolyte was a chloride-free 0.1 M citric acid solution buffered at pH 3 by titration with 1 M NaOH. All solutions were prepared from laboratory grade reagents and with high purity water of 18.2 M $\Omega$  cm (Millipore<sup>TM</sup> system). All experiments were repeated at least two times and exhibited very good reproducibility.

### 2.1. Gravimetric hydrogen collection measurements

Hydrogen collection measurements were conducted using the gravimetric method. Full details about this method, originally presented by Curioni [9], are given elsewhere [21]. The gravimetric method is based on the buoyant force exerted by hydrogen gas accumulated in a submerged container. For the case of anodic HE, this is the H<sub>2</sub> produced during Mg dissolution. The gravimetric method is extremely well suited for the study of anodic HE as it allows real-time hydrogen volume collection during polarization with higher sensitivity than the volumetric method [21].

Galvanodynamic polarization measurements were carried out on the HP Mg specimen scanning upwards from the open circuit potential (OCP) to a current density

of  $+75 \text{ mA cm}^{-2}$  at  $0.1 \text{ mA cm}^{-2} \text{ s}^{-1}$ . A Gamry Instruments Reference 600 potentiostat/galvanostat controlled by the Gamry Framework software was used to perform the electrochemical experiments.

A conventional three-electrode configuration was used in all electrochemical tests with the HP Mg sample acting as the working electrode, a Pt mesh as the counter electrode and a saturated calomel electrode (SCE) as the reference electrode. The OCP of the samples was monitored for about 10 minutes prior to the application of the polarization signals. This was the time needed by the system to reach a steady potential.

## 2.2. Scanning Vibrating Electrode Technique (SVET) measurements

In situ visualization and quantification of current density distributions over polarized Mg surfaces were performed using a SVET instrument of in-house construction, whose design and mode of operation are described in detail elsewhere [22]. The instrument employed a microprobe, consisting of a  $125 \text{ }\mu\text{m}$  diameter Pt wire encased within a glass sheath, that was vibrated at a frequency of 140 Hz and an amplitude of  $\pm 15 \text{ }\mu\text{m}$ . Calibration was carried out using a two compartment cell containing the relevant test electrolyte, as described previously [22], which enabled the SVET peak-to-peak voltage signal to be converted to values of current density along the axis of probe vibration ( $j_z$ ). SVET scans were performed at a constant height of  $100 \text{ }\mu\text{m}$  above the metal surface. SVET measurements were performed during galvanostatic polarization of the HP Mg electrode at 4 different anodic current densities in the range of 1 to  $10 \text{ mA cm}^{-2}$  by means of an in-house micro-galvanostat after about 10 min at the OCP. Even though the potential was not monitored under open circuit conditions, this was the time needed for the potential to reach a steady value as was observed in the gravimetric measurements. The samples used for SVET measurements were masked

with 90  $\mu\text{m}$  thick extruded PTFE 5490 tape (3M Ltd), such that only about  $5\times 5$  mm square area was exposed to electrolyte. The evolution of the time-dependent area-averaged cathodic current density ( $i_c$ ) during the time of galvanostatic current density application was determined using a procedure described in detail elsewhere [13, 22]. In brief, numerical area integration of  $j_z$  distributions was carried out for each scan to calculate the time-dependent total measured cathodic current ( $I_c$ ), which was then normalized by dividing by the nominal electrode surface area.

### *2.3. Cathodic potentiodynamic polarization of Mg after anodic polarization*

Cathodic potentiodynamic polarization curves after prior anodic dissolution have proven to be a reliable way to investigate the catalytic properties for the HER of previously polarized Mg surfaces. This approach, originally proposed by Birbilis et al. and Taheri et al. in parallel investigations [10, 19], was recently used to accurately determine the contribution of the corrosion film and accumulated impurities to the total HE rate on Mg electrodes of different purities in NaCl containing solutions [3, 5]. For that purpose, it was proposed that, immediately after the end of the anodic galvanostatic experiment, the influence of the corrosion product and enriched impurities on the electrode surface remains relatively unchanged during subsequent cathodic polarization. It was further assumed that this influence on the cathodic polarization curve reflects the effects of corrosion product and enriched impurities on the HER during the prior anodic treatment. This hypothesis was proven to be valid for the case of dissolving Mg [5]. The cathodic polarization curves were carried out immediately after the anodic galvanodynamic experiments. For these experiments, the electrolyte was replaced by fresh chloride-free 0.1 M citric acid buffer solution (pH 3) and the cathodic polarization

measurement was performed by scanning downwards 700 mV from the OCP at 1 mV/s. The sample was not rinsed between galvanodynamic and potentiodynamic experiments.

### 3. Results and discussion

#### 3.1. Gravimetric hydrogen collection measurements

Fig. 1a shows the rate associated with HE during anodic galvanodynamic polarization for the HP Mg electrode in 0.1 M citric acid buffer (pH 3) solution using the gravimetric method plotted as a function of the applied anodic current density. Results from triplicate experiments are shown, exhibiting a very good reproducibility. The reason for the noise observed in the curves is that it was calculated from the slope of consecutive individual weight measurements recorded at a small time scale. As a result, even small fluctuations in the buoyant force during dynamic polarization (i.e. convection in the electrolyte resulting from the intense evolution of H<sub>2</sub> gas) impact the HE current density signal. Fig. 1b shows the smoothed data for one of the curves where the noisy fluctuations were reduced by the Savitzky-Golay filtering method [23]. In this approach the signal-to-noise ratio is increased by fitting successive sub-sets of adjacent data points with a low-degree polynomial by the least squares method. Curves in Fig. 1a were smoothed using a second-order polynomial function with the aim of reducing the distortion of the original data. Due to their excellent reproducibility, only one curve in Fig. 1b is shown. A clear trend is exhibited with the HE current density increasing linearly over the whole range of applied anodic current densities, which confirms the occurrence of anodic HE in acidic media. Linear regression of the noisy curves showed that the anodic HE current density is  $55\pm 1\%$  of the applied current density. This value is about 10% lower than that observed for the same HP Mg material in unbuffered 0.1 M



NaCl solution [21]. It is worth noting in Fig. 1 the large HE rate exhibited at the OCP (zero applied current), indicating a very high corrosion rate of about  $15 \text{ mA cm}^{-2}$ .

Fig. 2 shows the HE rate during anodic galvanodynamic polarization experiments from Fig. 1 over the range from 0 to  $+10 \text{ mA cm}^{-2}$ . Individual values of the HE rate were determined by interpolation in the HE rate vs. applied current density plots in Fig. 1. The smoothed curves of the noisy data in Fig. 1a were used. This protocol was proven to be valid as reported in a previous study using the gravimetric method for  $\text{H}_2$  collection [21] where real-time HE rate during galvanodynamic polarization exhibited comparable values to those determined by galvanostatic experiments, providing complete information of anodic HE rate over a range of applied current density values of interest. The trend exhibited in Fig. 1 with HE rates increasing linearly with increased applied anodic current densities is confirmed. The same protocol was followed over the whole range of applied current densities (i.e. from 0 to  $+75 \text{ mA cm}^{-2}$ ) and linear regression of the interpolated HE rates resulted in the same relationship between the HE rate and  $i_{\text{app}}$  as that for the raw noisy data (i.e.  $55 \pm 1\%$  with a correlation coefficient of 0.998), which validates the application of the Savitzky-Golay filtering method.

It is interesting to note that, in contrast to results reported in a previous study [24], this behavior was also exhibited in the lowest applied current density regime (i.e. from 0 to  $+10 \text{ mA cm}^{-2}$ ). Rossrucker et al. investigated the evolution of anodic  $\text{H}_2$  on a Mg specimen of comparable purity using the same acidic buffer solution at identical conditions of concentration and pH (i.e. 0.1 M and pH 3) and no net increase of the HE rate was exhibited over a variety of current densities ranging from 0 to  $+10 \text{ mA cm}^{-2}$  [24]. Furthermore, decreased HE rates from that exhibited at the OCP were shown for the lowest anodic current densities applied [24]. Fig. 2 also shows the results from

Rossrucker et al. [24] for comparative purposes. Clear differences are observed as the HE rates obtained using the gravimetric method were about 1.5-2X lower than those reported by Rossrucker et al. [24]. The reason for this is unknown. However, it is interesting to note that while experiments in [24] were performed galvanostatically and the HE rate was measured volumetrically, the results in the present study used galvanodynamic polarization coupled with the gravimetric method for H<sub>2</sub> collection. It is possible that these differences and the better resolution of the gravimetric method for the HE rate determination [21] may be the cause for this behavior. Furthermore, a continuous increase in the HE rate was exhibited and no regions of decreased rates were shown. It is also worth noting that in the previous work [24] the HE rate exhibited its highest value at zero applied current (i.e. OCP), even higher than at +10 mA cm<sup>-2</sup>, whereas in the present investigation the HE rate was the lowest at the OCP and increased monotonically with increasing potential.

Fig. 3a shows the macroscopic surface appearance of one HP electrode surface after galvanodynamic anodic polarization measurements shown in Fig. 1. A very similar appearance was exhibited in all cases. Following polarization, the surface was roughened as a result of the uniform dissolution attack, but there was no evidence of dark corrosion product commonly found following polarization in other solutions [3, 5, 9, 10, 19, 25, 26]. Instead, a characteristic reflective metallic surface was exhibited (Fig. 3b). This confirms that the evolution of anodic H<sub>2</sub> is possible without the presence of this corrosion film. This observation is in agreement with a recent study where the primary source of H<sub>2</sub> evolution on dissolving ultra-high purity Mg polarized at anodic potentials was investigated [5]. In that work, evidence was provided that, even though the dark corrosion product exhibits enhanced catalytic activity towards the HER, the

evolution of hydrogen on dissolving ultra-pure Mg is primarily associated with the actively dissolving regions of the surface.

### 3.2. Scanning Vibrating Electrode Technique (SVET) measurements

Figs. 4-7 show typical SVET-derived surface maps of local current density along the axis of probe vibration ( $j_z$ ) above a UHP Mg surface during the galvanostatic application of anodic current densities of 1, 3, 5 and 10 mA cm<sup>-2</sup>, respectively, in 0.1 M chloride-free citric acid buffer (pH 3) solution as a function of time. Although the majority of the surface exhibited a net anodic activity associated with the dissolution reaction of the HP Mg electrode, some net cathodic current density was detected by the SVET during anodic polarization. Note that the SVET senses the net current above the sample. Consequently, any local cathodic current occurring at a region dominated by net anodic dissolution will remain unrevealed. In contrast with previous studies in NaCl solution where net cathodic activity corresponded with the corrosion product resulting from Mg dissolution [5, 13], the net cathodes in acidic buffer solution did not seem to correspond with any visually detectable feature on the surface. Furthermore, the cathodic activity detected during anodic polarization seemed to exhibit an on/off switching behavior. Net cathodes that appeared on the surface subsequently deactivated and evolved to net anodes coupled with simultaneous activation of new net cathodic sites located at different positions on the electrode surface. Interestingly, the presence of cathodic activity detected decreased as the applied anodic current density increased, as expected from standard electrochemical kinetics but opposite to the increased rate of HE measured gravimetrically. When a current density of +10 mA cm<sup>-2</sup> was applied to the HP Mg electrode, the surface exhibited a purely net anodic behavior with no visible net cathodes as shown in Fig. 7.

Fig. 8 shows the surface appearance of the HP Mg electrode after the SVET measurements at different anodic current densities. No evidence of the typical dark corrosion product typically exhibited in unbuffered chloride-containing solution was observed as similar surface appearance to that after galvanodynamic polarization was exhibited. This further supports the notion that the dark corrosion film deposited on the electrode surface in NaCl solution is not responsible for the enhanced HE rates exhibited under anodic polarization [3, 5]. Furthermore, it suggests that, (as also observed in Fig. 3) even though the experiments were carried out in a quiescent electrolyte, the buffer capacity of the acidic solution was not overwhelmed during polarization.

The SVET data in Figs. 4-7 were numerically integrated using the approach described elsewhere [13, 22]. This protocol allows for the time-dependent total measured anodic and cathodic current densities for each scan to be determined. Fig. 9 shows the SVET-derived integrated anodic and cathodic current density values (i.e.  $i_{\text{anod}}$  and  $i_{\text{cathod}}$ , respectively) emerging from the HP Mg surface in a chloride-free 0.1 M citric acid buffer solution under anodic galvanostatic polarization at different current densities plotted as a function of time. In contrast with previous observations of HP Mg in NaCl, neither the cathodic nor the anodic integrated current densities exhibited a clear increase with the time of polarization at any applied anodic current [5, 13]. Recall that no dark corrosion film deposited on the surface during anodic polarization (Figs. 3 and 8). Furthermore, the SVET-derived net cathodic currents actually exhibited lower values at a given time as the applied current density increased, as will be shown in more detail below. It is worth noting that, as the applied current density increased, a fraction of the electrochemical activity occurring above the dissolving HP Mg surface was underestimated by the SVET as exemplified by the lower values measured of  $i_{\text{anod}}$

compared with  $i_{\text{appl}}$ . It is likely that, given the low conductivity of the citric acid buffer solution, the detection efficiency of the SVET was reduced by perturbations in the ionic strength close to the electrode surface as a result of the dissolution process. Note that the SVET measures the ohmic potential drop between the peak-to-peak vibration amplitude of the probe. By Ohm's law, the peak-to-peak voltage signal ( $V_{\text{pp}}$ ) is converted to current flux density along the axis of probe vibration ( $j_z$ ) by:

$$V_{\text{pp}} = j_z (a_{\text{pp}} / \kappa) \quad (1)$$

where  $a_{\text{pp}}$  is the peak-to-peak vibration amplitude and  $\kappa$  is the electrolyte conductivity. The SVET calibration factor ( $G$ ) is defined as  $G=(\kappa/a_{\text{pp}})$  [22]. Full details of the SVET calibration procedure are given elsewhere [22]. Considering that the calibration factor used to convert  $V_{\text{pp}}$  to  $j_z$  was determined using two Pt electrodes, local increase in the solution conductivity due to Mg dissolution may have led to higher values of  $G$  in comparison to that determined during the calibration procedure. This resulted in an apparent lowering in the magnitude of the calculated current density values detected (i.e. lower values of  $i_{\text{anod}}$  compared to  $i_{\text{appl}}$ ). At applied anodic current densities of 3 and 5 mA cm<sup>-2</sup>, this artifact caused an underestimation of the electrochemical activity lower than or equal to 20%. However, the underestimation was about 50% for the highest applied anodic current density (i.e. +10 mA cm<sup>-2</sup>). Fig. 10 shows the SVET-derived integrated cathodic current density values ( $i_{\text{SVET}}$ ) taken from Fig. 9 together with the total cathodic current densities associated with HE calculated measured using the gravimetric method ( $i_{\text{TOT}}$ ) plotted as a function of time. It should be mentioned that the  $i_{\text{TOT}}$  values were calculated by converting the HE rates obtained during the galvanodynamic polarization measurements (see Fig. 2b) using Faraday's law. As observed,  $i_{\text{TOT}}$  increased with increasing the anodic current density applied whereas  $i_{\text{SVET}}$  presented the opposite behavior, exhibiting lower values as higher anodic current

densities were applied. In a previous work where the evolution of anodic  $H_2$  was investigated in unbuffered NaCl solution, it was shown that the net cathodic currents detected by the SVET were associated with enriched impurities and the dark corrosion film deposited on the electrode surface [5]. The corrosion film, as reported by other authors [9, 12], was confirmed to exhibit enhanced catalytic activity for the HER [5]. In other words, the dark corrosion film formed during anodic polarization of Mg promotes the evolution of anodic  $H_2$  at a faster rate. In acidic conditions like those used in the present investigation, the formation of this oxide/hydroxide corrosion product [19] is not thermodynamically favored and, consequently, it is expected that no net cathodic activity should be detected on the anodically polarized HP Mg surface. It is possible that the few regions of the surface exhibiting net cathodic activity (see Figs. 4-7) were due to transients of corrosion product that may have formed as a consequence of local alkalization of the electrolyte close to the electrode surface resulting from the HER. The intense convection in the electrolyte originated by the copious HE would result in replacement of local alkaline environments with the bulk buffered solution, restoring the acidic pH conditions above the surface and dissolving these deposits shortly after formation. This view is consistent with the on/off behavior observed for the local net cathodes shown in Figs. 4-7.

Despite the near absence of SVET-detected net cathodic activity on the HP Mg surface during anodic polarization as shown in Fig. 10, enhanced rates of HE were measured gravimetrically as the applied anodic current density increased, Fig. 1. Furthermore, Fig. 10 shows that at least 3 orders of magnitude difference between  $i_{TOT}$  and  $i_{SVET}$  were observed for any given applied anodic current density. This suggests that almost the entire cathodic activity remained undetected. Since the SVET senses current flowing to distant cathodes, either on the working electrode surface or the remote

counter electrode, it is likely that most of the cathodic regions on the anodically polarized surface were masked by the net anodic behavior exhibited by the electrode during dissolution. In other words, the cathodes were either closely located or co-located with the anodes. Furthermore, the SVET can only detect current flowing to locations on the order of the distance equal to the SVET probe scan height (100  $\mu\text{m}$  in the present work). Consequently, current flux lines coupling anodic Mg dissolution with local cathodic HE will pass well below the plane of scan and as such remain undetected by SVET (schematic diagrams illustrating this situation can be found elsewhere [27]). In any case, the results clearly show that, in the absence of the dark corrosion film observed in NaCl solution, the evolution of  $\text{H}_2$  under anodic polarization of a high purity Mg surface occurs almost entirely at the regions dominated by the anodic dissolution reaction. In other words, the large majority of the anodic HE originates at net anodic sites.

### *3.3. Cathodic potentiodynamic polarization of Mg after anodic polarization and the effect of noble impurity concentration*

Fig. 11 shows the cathodic potentiodynamic polarization curves of the previously anodically polarized HP Mg surfaces in chloride-free 0.1 M citric acid buffer solution. Experiments were carried out right after anodic galvanodynamic polarization measurements up to  $+75 \text{ mA cm}^{-2}$  were finished. Prior to cathodic polarization the electrolyte was replaced by fresh chloride-free 0.1 M citric acid buffer solution to avoid any influence on the local pH that prior anodic polarization may have caused. Cathodic polarization curves on a freshly polished HP Mg surface in chloride-free 0.1 M citric acid buffer solution with no prior anodic treatment are also presented for comparative purposes. Results from duplicate experiments are presented and a very good

reproducibility is observed. This protocol, used in previous works [3, 5, 6, 12] and originally developed by Birbilis et al. [10] and Taheri et al. [19], allows for the catalytic activity for the HER of previously corroded Mg surfaces to be examined.

As shown in Fig. 11, no evidence of enhanced cathodic kinetics was exhibited by the corroded surfaces after anodic polarization of the HP Mg in acidic buffer solution. However, the shifting of the  $E_{\text{corr}}$  towards more positive values suggests that after dissolution the anodic kinetics were slightly suppressed. This anodic deactivation was recently reported for an ultra-high purity Mg specimen in 2 M NaCl where the typical dark corrosion product formed on the electrode surface [5]. However, in the present investigation no visible corrosion product that may partially protect the HP Mg surface was observed (see Fig. 3). Thomas et al. [15] investigated the effect of Fe concentration on Mg dissolution in 0.1 M NaCl and found that, along with cathodic activation, galvanostatic anodic polarization also caused anodic activation of the Mg sample. Increased dissolution rates were seen for Fe concentrations in the Mg specimen equal and greater than 220 ppmw. However, for an Fe concentration of 25 ppmw (similar to that of the HP Mg used in the present investigation) negligible enhanced dissolution rates were observed. A dark filiform-like corrosion product formed in all cases. It is interesting that in acidic conditions and in the absence of any visible corrosion film, deactivation of anodic kinetics was exhibited by previously polarized Mg surfaces.

The unchanged cathodic kinetics after anodic dissolution of the HP Mg surface provides evidence of a negligible accumulation of noble impurities on the surface during dissolution. Furthermore, it also indicates that Fe re-deposition did not occur to an extent that affected the HE behavior. If Fe was enriched or re-plated, enhanced cathodic activity should be exhibited after dissolution whereas no evidence of any



cathodic enhancement is observed. This finding contradicts interpretations to explain the evolution of anodic  $H_2$  on dissolving Mg based on the accumulation of noble metal impurities on the corroded surface [14, 16, 19] and Fe re-deposition [20]. It is possible that the Fe cations resulting from the free-corrosion of Fe impurities released to the electrolyte may have been complexed by the citrate ions present in the buffer solution. Furthermore, the chelate effect provides large stability constants for the formation of these complexes, poisoning Fe-ion re-deposition [28]. Nonetheless, the enhanced rates of HE observed during anodic polarization indicate that further work is needed to understand the effects of noble metal re-deposition on anodic  $H_2$ .

#### *3.4. Notional model for the evolution of anodic hydrogen*

The results presented in this work together with those presented in a previous study [5], allows for elucidation of a notional model for the evolution of anodic  $H_2$ . The role in the process of the three possible sources for anodic HE will be briefly summarized.

##### a) The role of the corrosion film:

The enhanced catalytic activity exhibited by the corrosion product formed during dissolution of Mg in neutral and alkaline solutions has been described in several studies [3, 9, 12, 13, 19, 25]. However, recent investigations [5] confirmed that despite the greater ability of the corrosion film to support the HER compared with the fresh uncorroded Mg surface, its effect in the total amount of  $H_2$  gas evolved at anodic polarization is small and decreases with increasing polarization above the OCP. Furthermore, the results presented here show that anodic HE is still exhibited in acidic solutions, where no evidence of this corrosion product was found. In other words, although the dark corrosion film plays a role at open circuit and contributes to

the total HE at anodic conditions, it is not necessary for this phenomenon to occur and, when present, it is responsible for only a small fraction of the anodic H<sub>2</sub> gas evolved.

b) The role of noble metal impurities:

Accumulation of impurities more noble than Mg during anodic dissolution has been found to occur at a very low extent with enrichment efficiencies lower than 1% [14-17]. Furthermore, gravimetric H<sub>2</sub> collection measurements on an UHP Mg specimen with concentration of impurities in the bulk metal of about 1 ppmw in NaCl solution, where the accumulation of impurities can be reasonably neglected, showed that the rate of HE increased remarkably with anodic polarization [3, 5]. These findings confirm that, even if the accumulation of noble impurities on the electrode surface occurs and may contribute to a very low extent, this mechanism is not responsible for the enhanced rates of HE in Mg subjected to anodic polarization. Further attention deserves the possible effect of self-corroded noble metal re-plating during polarization. This mechanism might also increase the HE and thus corrosion rate under open circuit conditions, but it is unlikely that this process plays a major role in the persistent HE exhibited on Mg at anodic potentials. In any case, more experiments are needed to fully understand the possible effect of this mechanism during anodic polarization.

c) The role of the dissolving anodic regions:

Previous studies have shown that dissolving anodic regions are the primary source for anodic HE on dissolving Mg [3, 5]. Frankel et al. [4] proposed an alternative explanation for the evolution of anodic hydrogen based in the increased catalytic activity of the surface with increasing applied potential or current as embodied by increases in the exchange current density for the HE reaction on Mg

( $i_{0,H_2,Mg}$ ). This model considers  $i_{0,H_2,Mg}$  as a dynamic parameter instead of as a constant that changes due to anodic polarization. It is possible that, as proposed by others [30], increased anodic polarization could lead to more depassivated regions that may act as preferential sites for anodic HE, nominally increasing  $i_{0,H_2,Mg}$ . Yang et al. [30] investigated anodic HE on a Mg specimen of comparable purity to that used in the present paper by real time imaging of the corroding surface during anodic polarization in alkaline and neutral environments, and in the presence and absence of chloride ions. They proposed that local depassivation of the Mg surface promoted by the presence of chlorides and the anodic current provided by the potentiostat would create a film-free corrosion front with the bare metal surface and the electrolyte in direct contact. In such a case, increased values of the anodic current applied would enhance depassivation thus leading to increased rates of anodic HE. Even though this model may explain the enhanced rates of HE under anodic polarization observed on dissolving Mg in neutral and alkaline environments, more experiments are needed to know if the surface is actually in direct contact with the electrolyte at any time or, on the contrary, a transient film exists on the anodic regions during polarization. Furthermore, this model is not consistent with the observations presented in this paper where, in acidic solution, the native oxide film is not thermodynamically stable and the dissolution process is shown to be uniform and not localized. It is also a possibility that changes in the interface between the specimen and the electrolyte due to anodic polarization may induce changes in the micro-electrochemical kinetic parameters involved in the process such as activation energy and/or rate constants favoring the HER under anodic dissolution. Taylor [31] recently proposed a mechanistic model using the density functional theory to analyze the reaction kinetics of the HER under anodic polarization using first-principle data. Rate constants

associated with the process were calculated and reasonable agreement in terms of the shape of a HER rate vs. applied potential/current density plot and order of magnitude of hydrogen evolved was observed. This model, however, still holds a lot of questions without clear answers [31].

Experimental evidence proved that the majority of the hydrogen that evolved under anodic polarization on Mg is associated with the actively dissolving anodes and, even though the reasons for increased values of  $i_{0,H_2,Mg}$  with the amount of polarization are not clear yet and more experiments are needed to fully understand the nature of the process, this explanation accounts for the enhanced HE current densities exhibited when anodic currents are applied, which is the sign of a strong enhancement in the catalytic activity for the HER in the anodic region

#### 4. Conclusions

Galvanodynamic measurements coupled with real-time gravimetric H<sub>2</sub> volume collection, SVET and potentiodynamic polarization experiments were carried out on high purity Mg (99.96% Mg) in chloride-free 0.1 M citric acid solution buffered at pH 3 to determine the source of anodic HE and to study the role of the film and the accumulation of noble impurities on the H<sub>2</sub> evolution kinetics upon anodic polarization. The following can be concluded:

- Anodic H<sub>2</sub> evolution still occurs in acidic solution with no evidence of the typical dark corrosion film formed in neutral and alkaline environment. Consequently, the occurrence of anodic HE is independent on the presence this corrosion product.
- The primary source of anodic HE is associated with regions dominated by the Mg anodic dissolution reaction. This is particularly evident as the applied anodic current density increases, where the electrode surface exhibited a purely net anodic activity

even though gravimetric H<sub>2</sub> collection showed increased values in the rate of anodic HE.

- **Cathodic polarization curves showed** no evidence of noble impurity enrichment or Fe re-deposition upon anodic **galvanostatic** polarization of the HP Mg electrode. The corroded surfaces did not exhibit **enhanced** cathodic activity after the anodic treatment was performed indicating that **for the anodic charge and period of time tested**, even if these processes may occur, they **did** not play a major role in the anodic HE.

### **Acknowledgements**

S. Fajardo expresses his gratitude to the State Research Agency (Ministry of Economy, Industry and Competitiveness of Spain), the Spanish National Research Council (CSIC) and the European Regional Development Fund (ERDF) for the financial support under the Project MAT2015-74420-JIN (AEI/FEDER/UE). G. Williams and C.F. Glover recognize the financial support of the EPSRC, Welsh Government and Innovate UK for the SPECIFIC Innovation and Knowledge Centre (grant numbers EP/I019278/1, EP/K000292/1, EP/L010372/1). The authors thank Nick Birbilis for supplying the HP Mg.

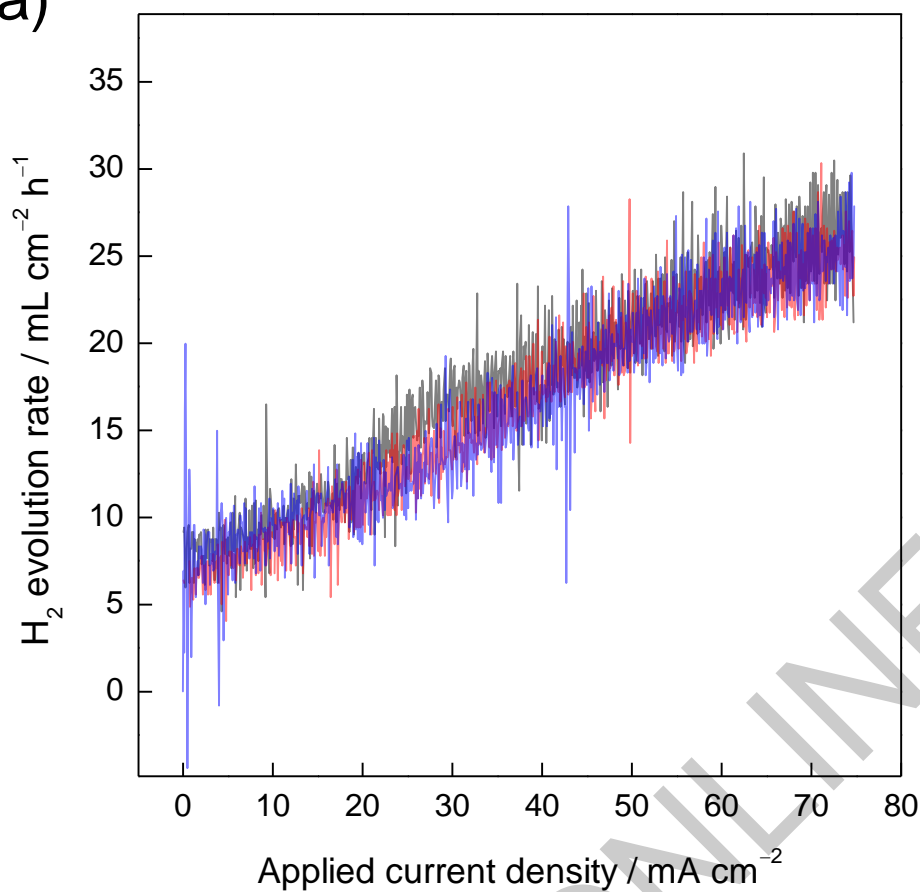
### **References**

- [1] S. Thomas, N.V. Medhekar, G.S. Frankel, N. Birbilis, *Curr. Opin. Solid State Mater. Sci.* 19 (2015): p. 85.
- [2] A. Atrens, W. Dietzel, *Adv. Eng. Mater.* 9 (2007): p. 292.
- [3] S. Fajardo, G.S. Frankel, *Electrochim. Acta* 165 (2015): p. 255.
- [4] G.S. Frankel, A. Samaniego, N. Birbilis, *Corros. Sci.* 70 (2013): p. 104.

- [5] S. Fajardo, C.F. Glover, G. Williams, G.S. Frankel, *Electrochim. Acta* 212 (2016): p. 510.
- [6] G.S. Frankel, S. Fajardo, B.M. Lynch, *Faraday Discuss.* 180 (2015): p. 11.
- [7] G.S. Frankel, The growth of 2-D pits in thin film aluminum, *Corros. Sci.* 30 (1990): p. 1203.
- [8] D.M. Dražić, J.P. Popić, *J. Appl. Electrochem.* 29 (1999): p. 43.
- [9] M. Curioni, *Electrochim. Acta* 120 (2014): p. 284.
- [10] N. Birbilis, A.D. King, S. Thomas, G.S. Frankel, J.R. Scully, *Electrochim. Acta* 132 (2014): p. 277.
- [11] G. Williams, N. Birbilis, H.N. McMurray, *Faraday Discuss.* 180 (2015): p. 313.
- [12] S.H. Salleh, S. Thomas, J.A. Yuwono, K. Venkatesan, N. Birbilis, *Electrochim. Acta* 161 (2015): p. 144.
- [13] G. Williams, N. Birbilis, H.N. McMurray, *Electrochem. Comm.* 36 (2013): p. 1.
- [14] D. Lysne, S. Thomas, M.F. Hurley, N. Birbilis, *J. Electrochem. Soc.* 162 (2015): p. C396.
- [15] S. Thomas, O. Gharbi, S.H. Salleh, P. Volovitch, K. Ogle, N. Birbilis, *Electrochim. Acta* 210 (2016): p. 271.
- [16] T. Cain, S.B. Madden, N. Birbilis, J.R. Scully, *J. Electrochem. Soc.* 162 (2015): p. C228.
- [17] N. Birbilis, T. Cain, J.S. Laird, X. Xia, J.R. Scully, A.E. Hughes, *ECS Electrochem. Lett.* 4 (2015): p. C34.
- [18] R.E. McNulty, J.D. Hanawalt, *ECS Transactions* 81 (1942): p. 423.
- [19] M. Taheri, J.R. Kish, N. Birbilis, M. Danaie, E.A. McNally, J.R. McDermid, *Electrochim. Acta* 116 (2014): p. 396.

- [20] D. Hoche, C. Blawert, S.V. Lamaka, N. Scharnagl, C. Mendis, M.L. Zheludkevich, *Phys. Chem. Chem. Phys.* 18 (2016): 1279.
- [21] S. Fajardo, G.S. Frankel, *J. Electrochem. Soc.* 162 (2015): p. C693.
- [22] G. Williams, H. Neil McMurray, *J. Electrochem. Soc.* 155 (2008): p. C340.
- [23] A. Savitzky, M.J.E. Golay, Smoothing and differentiation of data by simplified least squares procedures, *Anal. Chem.* 36 (1964): p. 1627.
- [24] L. Rossrucker, A. Samaniego, J.-P. Grote, A.M. Mingers, C.A. Laska, N. Birbilis, G.S. Frankel, K.J.J. Mayrhofer, *J. Electrochem. Soc.* 162 (2015): p. C333.
- [25] M. Curioni, F. Scenini, T. Monetta, F. Bellucci, *Electrochim. Acta* 166 (2015): p. 372.
- [26] S. Lebouil, O. Gharbi, P. Volovitch, K. Ogle, *Corrosion* 71 (2015): p. 234.
- [27] G. Williams, A.J. Coleman, H.N. McMurray, *Electrochim. Acta* 55 (2010): p. 5947.
- [28] M. Matzapetakis, C.P. Raptopoulou, A. Tsohos, V. Papaefthymiou, N. Moon, A. Salifoglou, *J. Am. Chem. Soc.* 120 (1998): p. 13266.
- [29] S.V. Lamaka, D. Höche, R.P. Petrauskas, C. Blawert, M.L. Zheludkevich, *Electrochem. Comm.* 62 (2016): p. 5.
- [30] Y. Yang, F. Scenini, M. Curioni, *Electrochim. Acta* 198 (2016): p. 174.
- [31] C. Taylor, *J. Electrochem. Soc.* 163 (2016): p. C602.

a)



b)

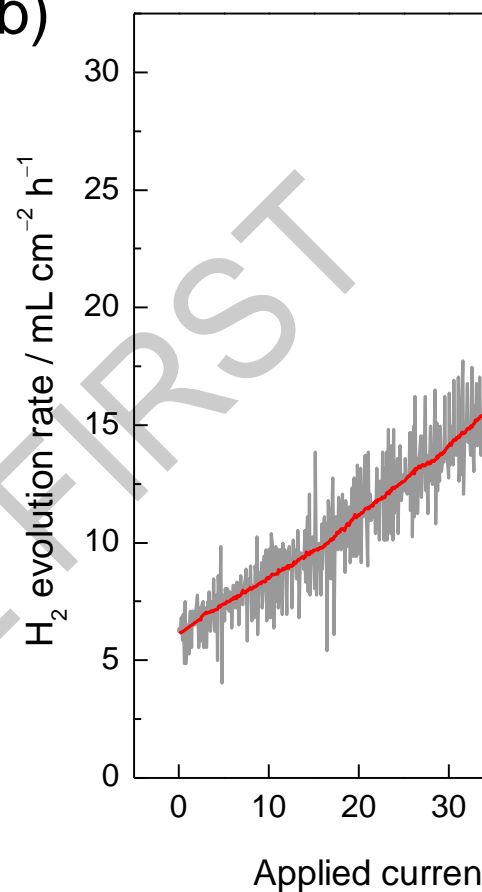


**Fig. 1.** Hydrogen evolution rate for the HP Mg electrode in 0.1 M Citric Acid buffer (pH 3) solution during a polarization as a function of the applied current density. HE current densities calculated from gravimetric measurements and galvanodynamic polarization. The scan rate was 0.1 mA/cm<sup>2</sup> s. Data from triplicate experiments are presented in order smoothed curve.



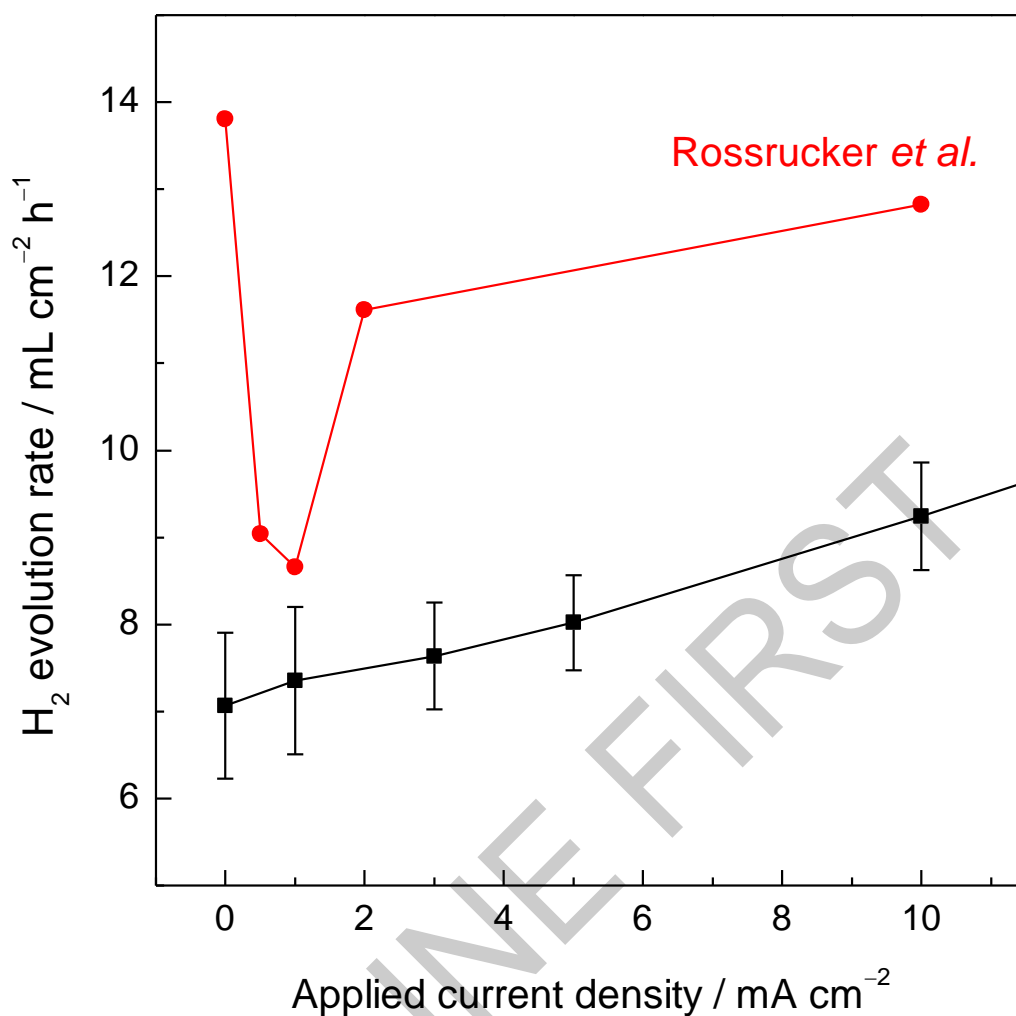
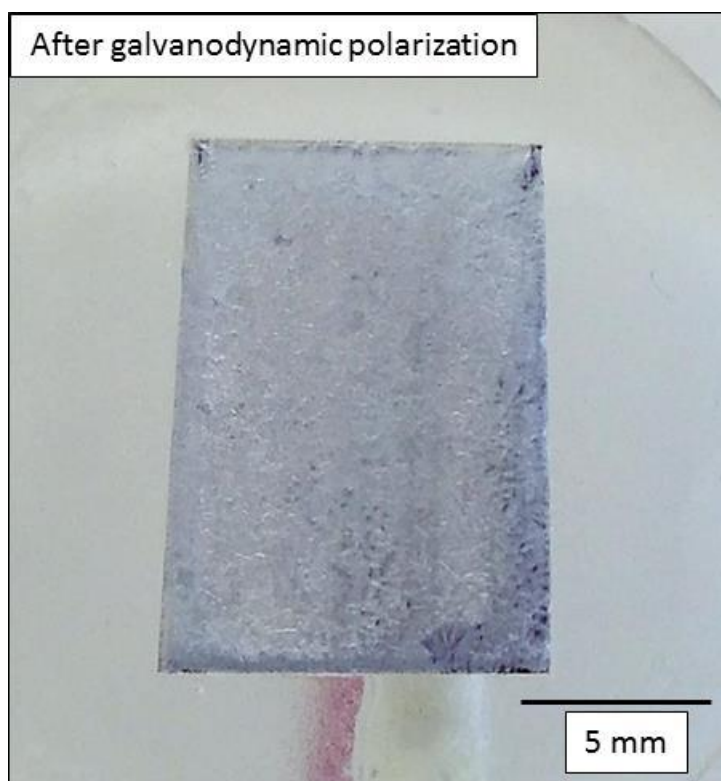
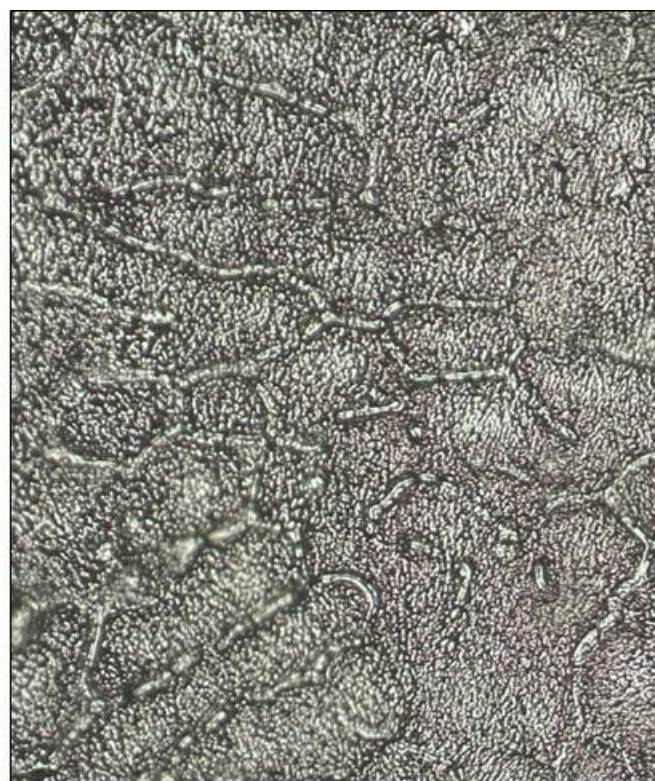


**Fig. 2.** Hydrogen evolution rate for the HP Mg electrode in 0.1 M Citric Acid buffer (pH 3) solution plotted as a function of the applied anodic current density. Hydrogen evolution rate was calculated by interpolation of data presented in Fig. 1. Results from Rossrucker et al. [24] included for comparative purposes. Error bars are standard deviation.



a)



b)

**Fig. 3.** Surface appearance of the HP Mg electrode after anodic galvanodynamic polarization in 0.1 M C solution using the gravimetric method for H<sub>2</sub> collection. Current density range from 0 to +75 mA c

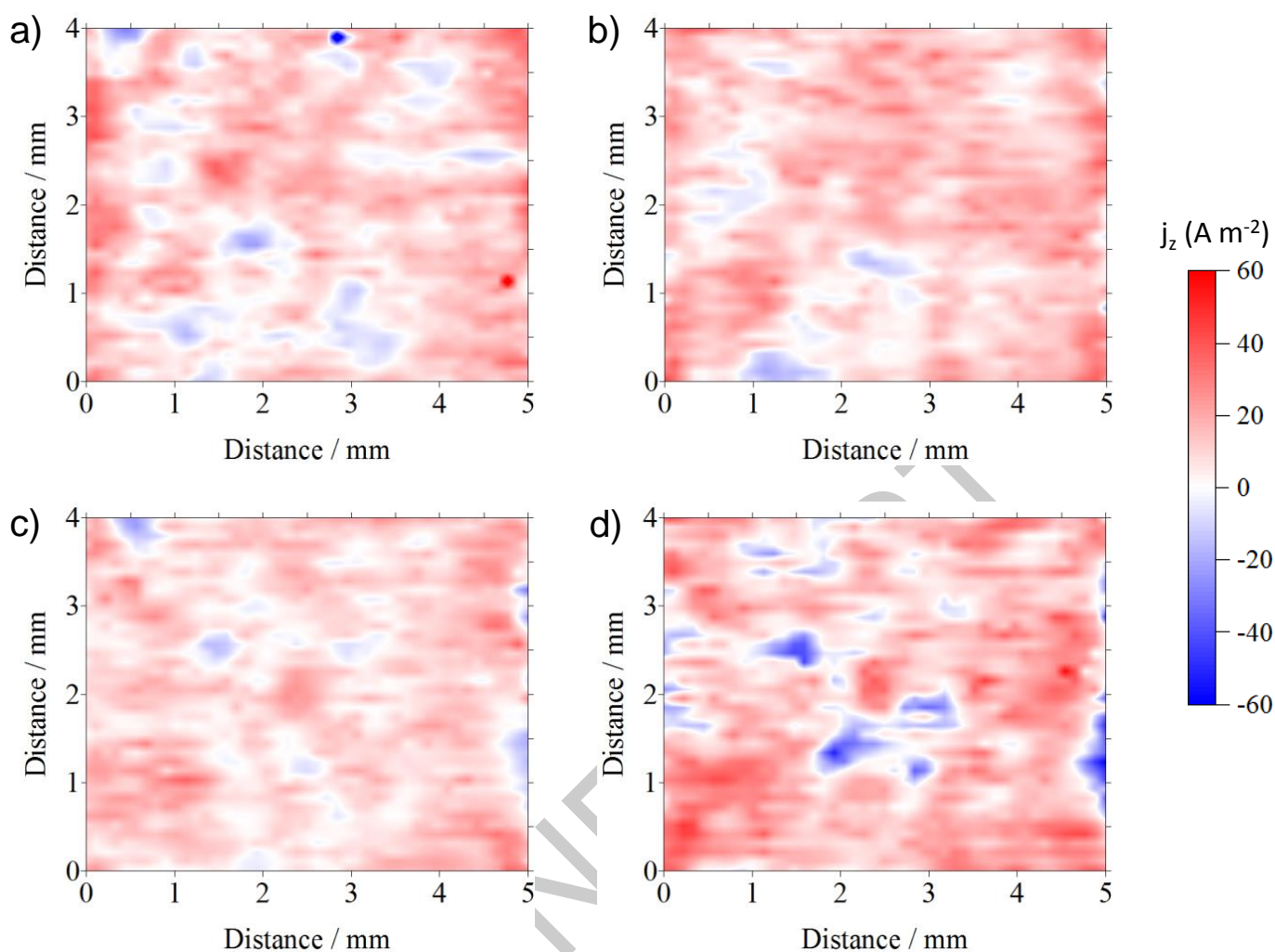


**Fig. 4.** Surface maps showing normal current density ( $j_z$ ) distributions above a HP Mg surface immersed in a 0.1 M Citric Acid buffer (pH 3) solution, (a) 8, (b) 32, (c) 48 and (d) 64 min after starting galvanostatic polarization at  $+1 \text{ mA cm}^{-2}$ .

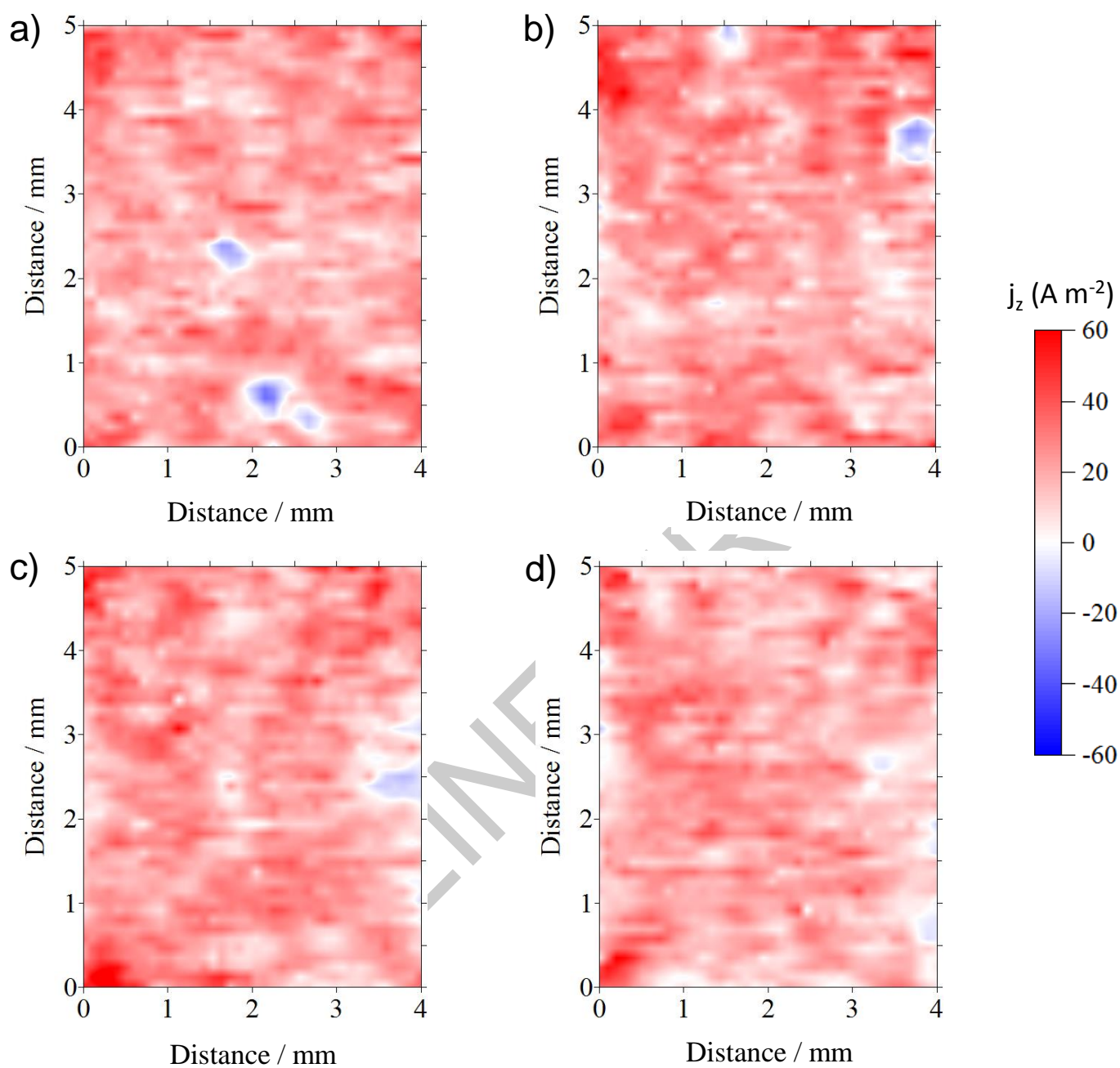


**Fig. 5.** Surface maps showing normal current density ( $j_z$ ) distributions above a HP Mg surface immersed in a 0.1 M Citric Acid buffer (pH 3) solution, (a) 8, (b) 32, (c) 48 and (d) 64 min after starting galvanostatic polarization at  $+3 \text{ mA cm}^{-2}$ .

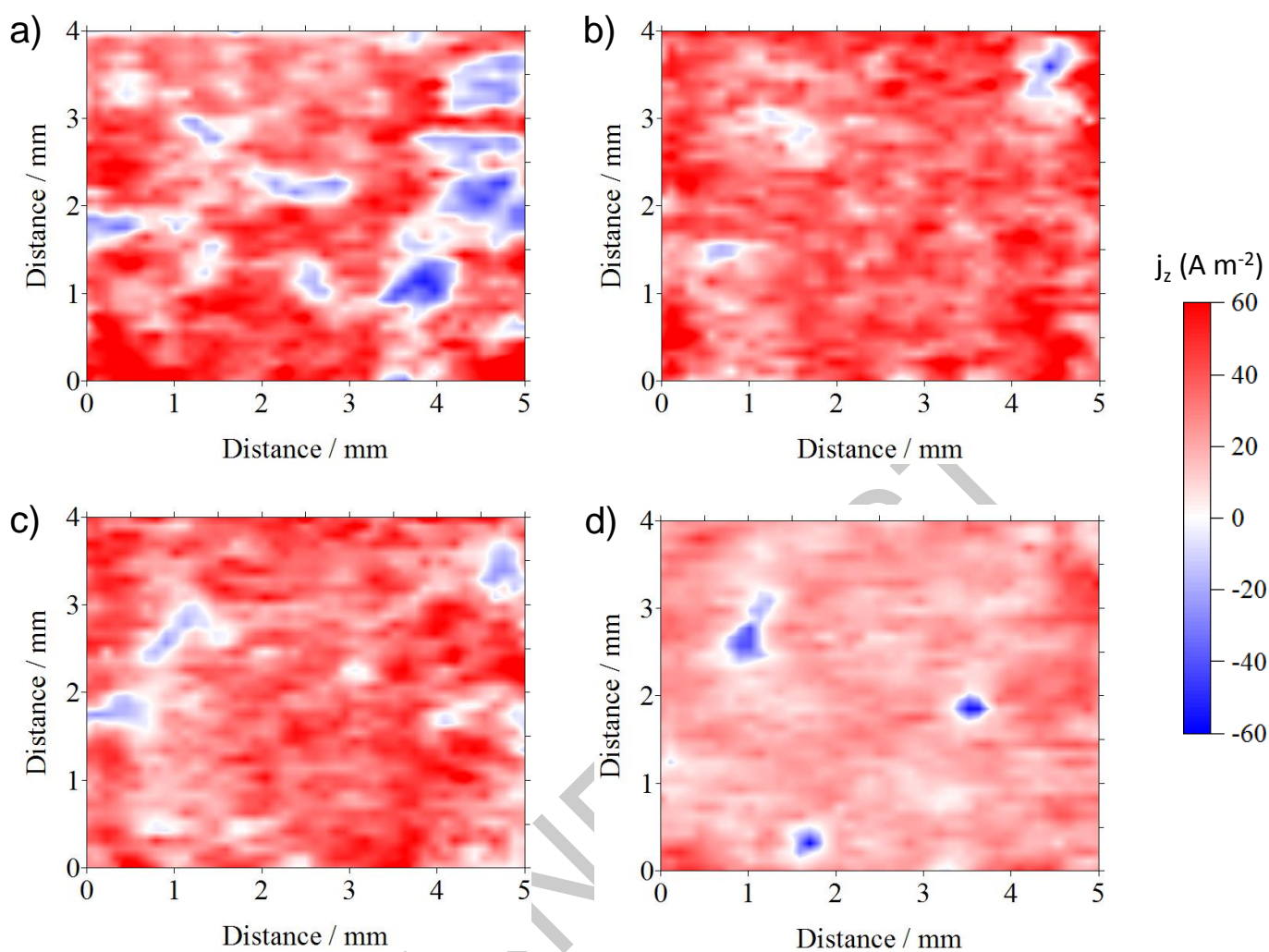


**Fig. 6.** Surface maps showing normal current density ( $j_z$ ) distributions above a HP Mg surface immersed in a 0.1 M Citric Acid buffer (pH 3) solution, (a) 7, (b) 28, (c) 49 and (d) 70 min after starting galvanostatic polarization at  $+5 \text{ mA cm}^{-2}$ .

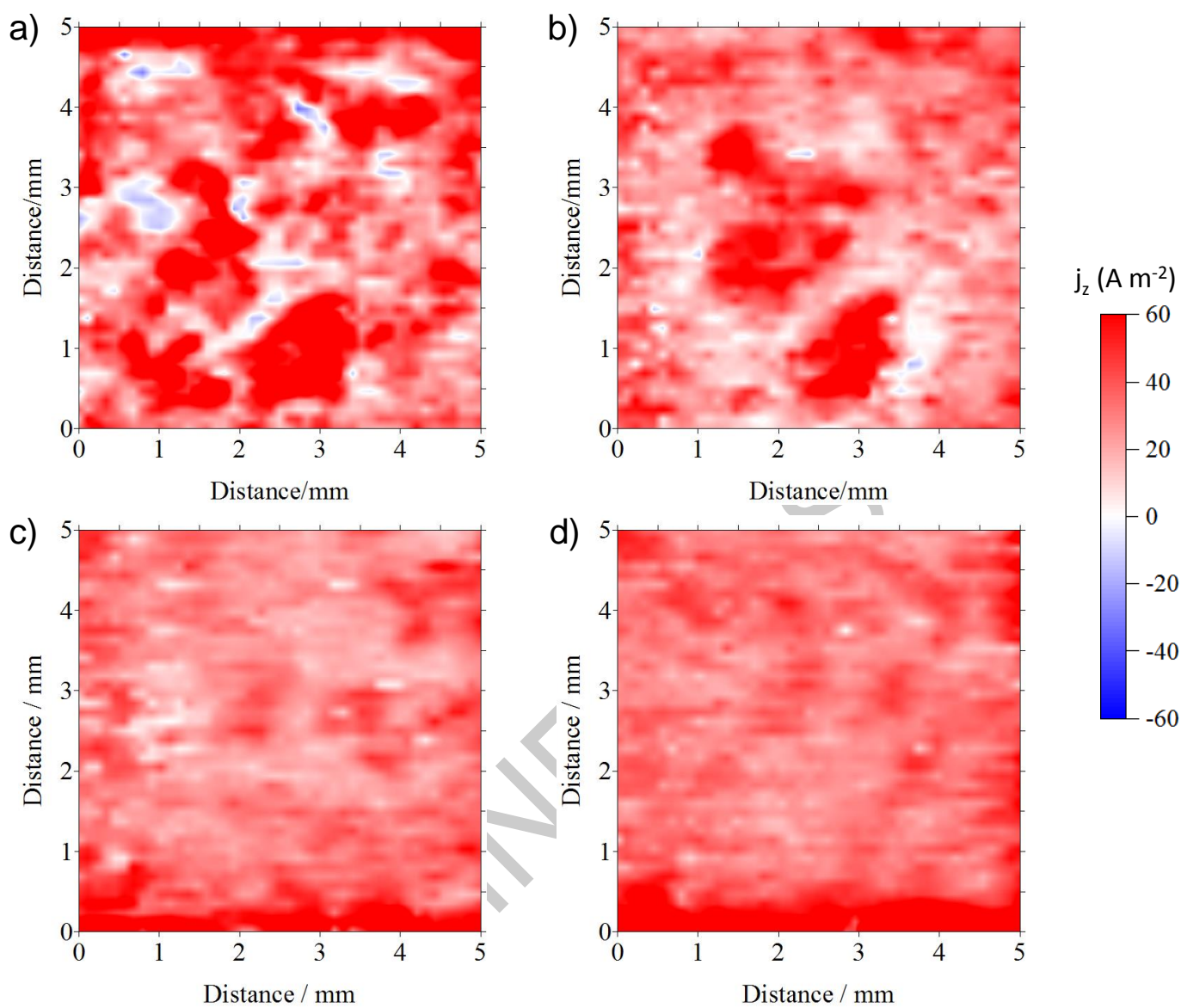


**Fig. 7.** Surface maps showing normal current density ( $j_z$ ) distributions above a HP Mg surface immersed in a 0.1 M Citric Acid buffer (pH 3) solution, (a) 7, (b) 28, (c) 49 and (d) 70 min after starting galvanostatic polarization at  $+10 \text{ mA cm}^{-2}$ .

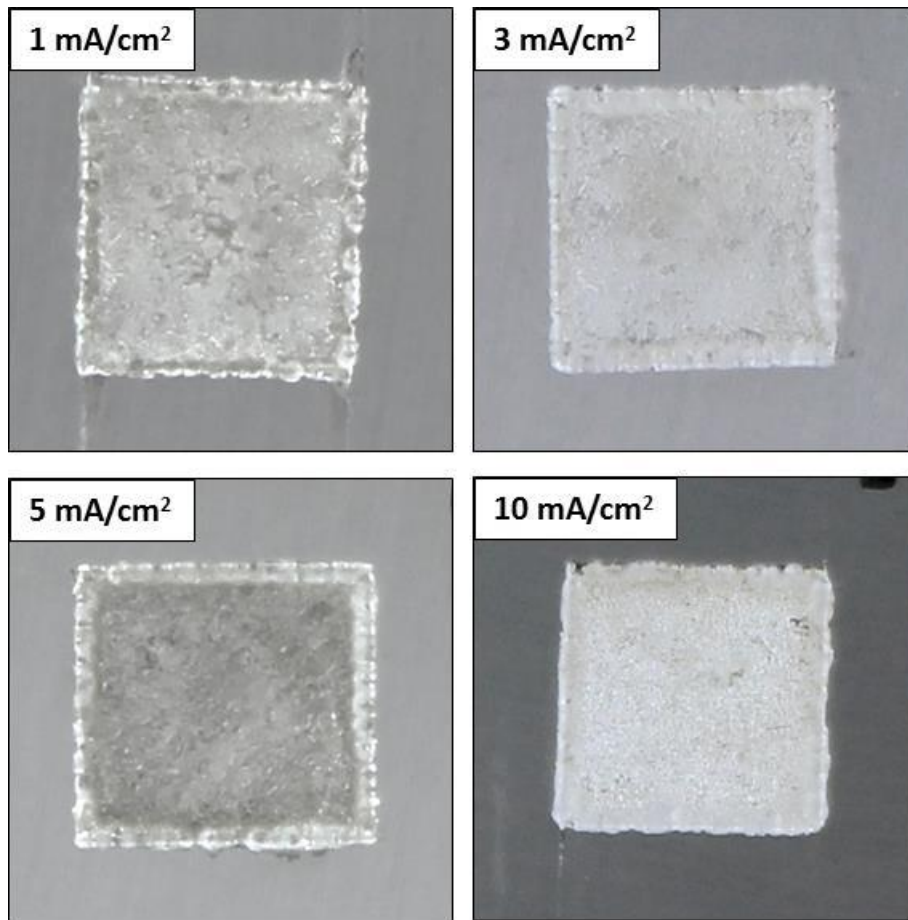


**Fig. 8.** Surface appearance of the HP Mg electrode after the SVET measurements where different anodic current densities were applied in 0.1 M Citric Acid buffer (pH 3) solution.

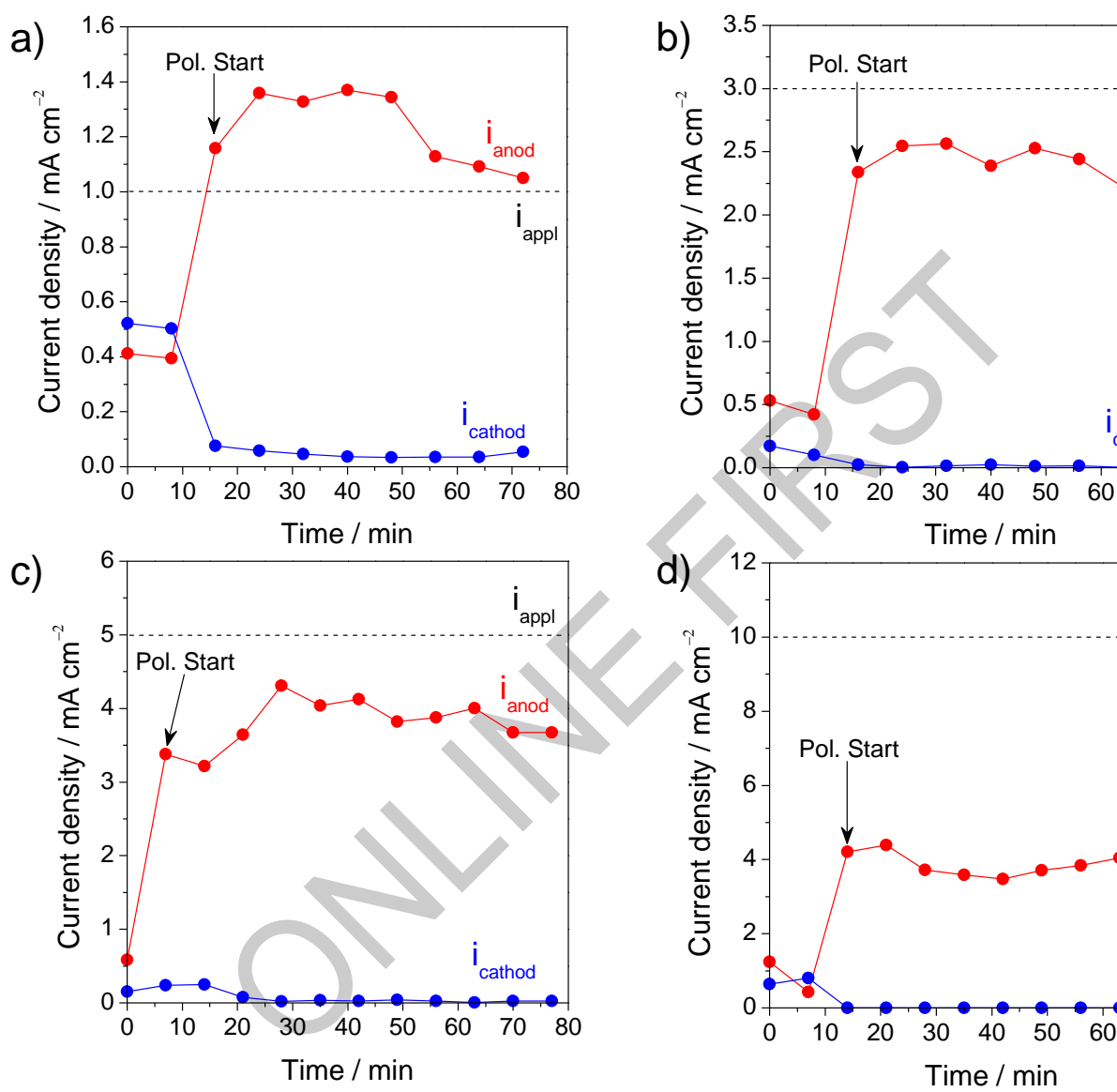


**Fig. 9.** SVET-derived integrated current density values emerging from a HP Mg surface under anodic galvanostatic polarization at a)  $3 \text{ mA cm}^{-2}$ , b)  $3 \text{ mA cm}^{-2}$ , c)  $5 \text{ mA cm}^{-2}$  and d)  $10 \text{ mA cm}^{-2}$  in 0.1 M Citric Acid buffer solution plotted as a function of time. Current density is presented as absolute value.



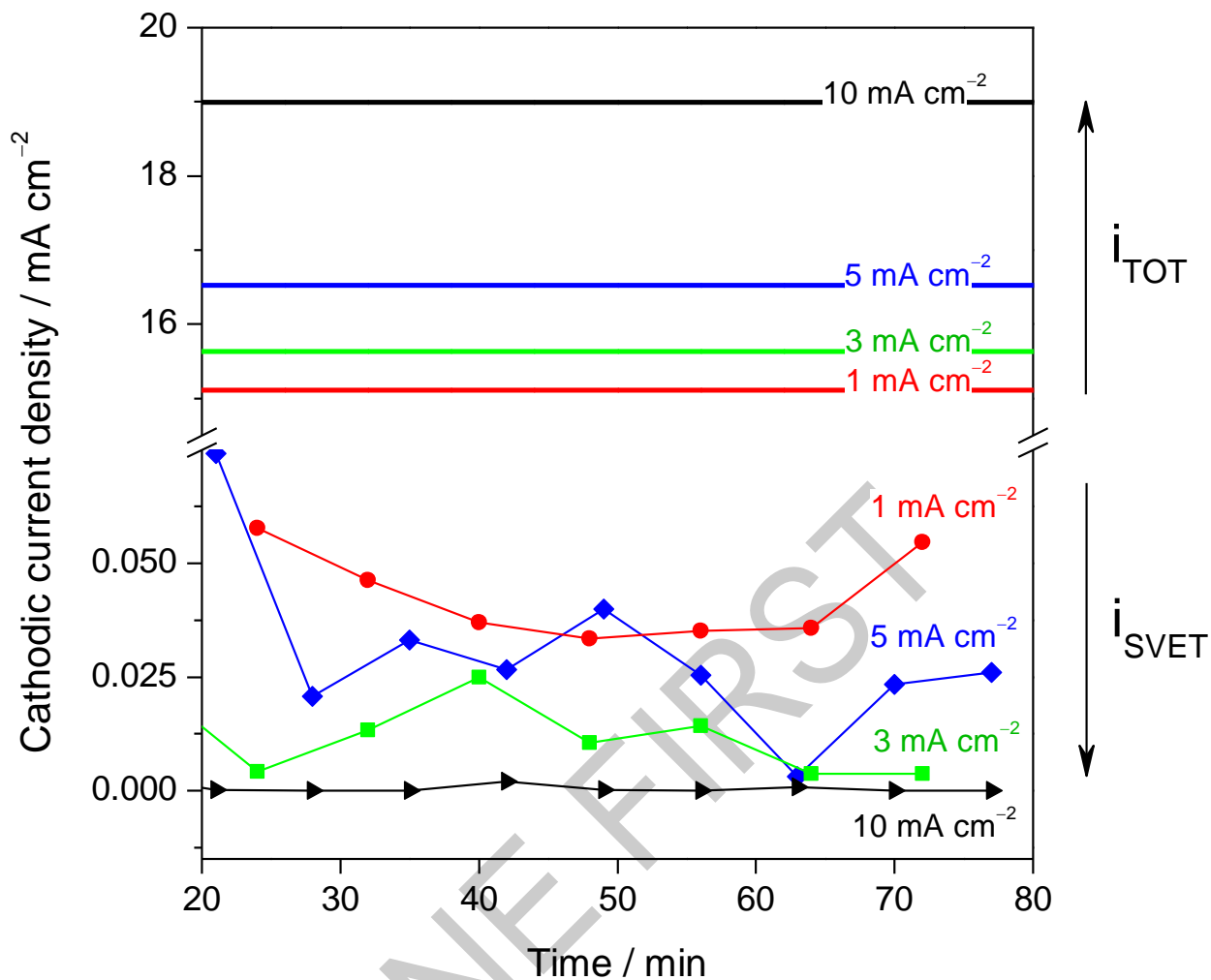


**Fig. 10.** SVET-derived integrated cathodic current density ( $i_{SVET}$ ) emerging from an HP Mg surface under galvanostatic polarization at different anodic current densities in 0.1 M Citric Acid buffer (pH 3) solution plotted as a function of time. Solid lines are the current density associated with HE ( $i_{TOT}$ ) obtained using the gravimetric method. Current density was calculated using Faraday's Law. Current density is presented as absolute value.

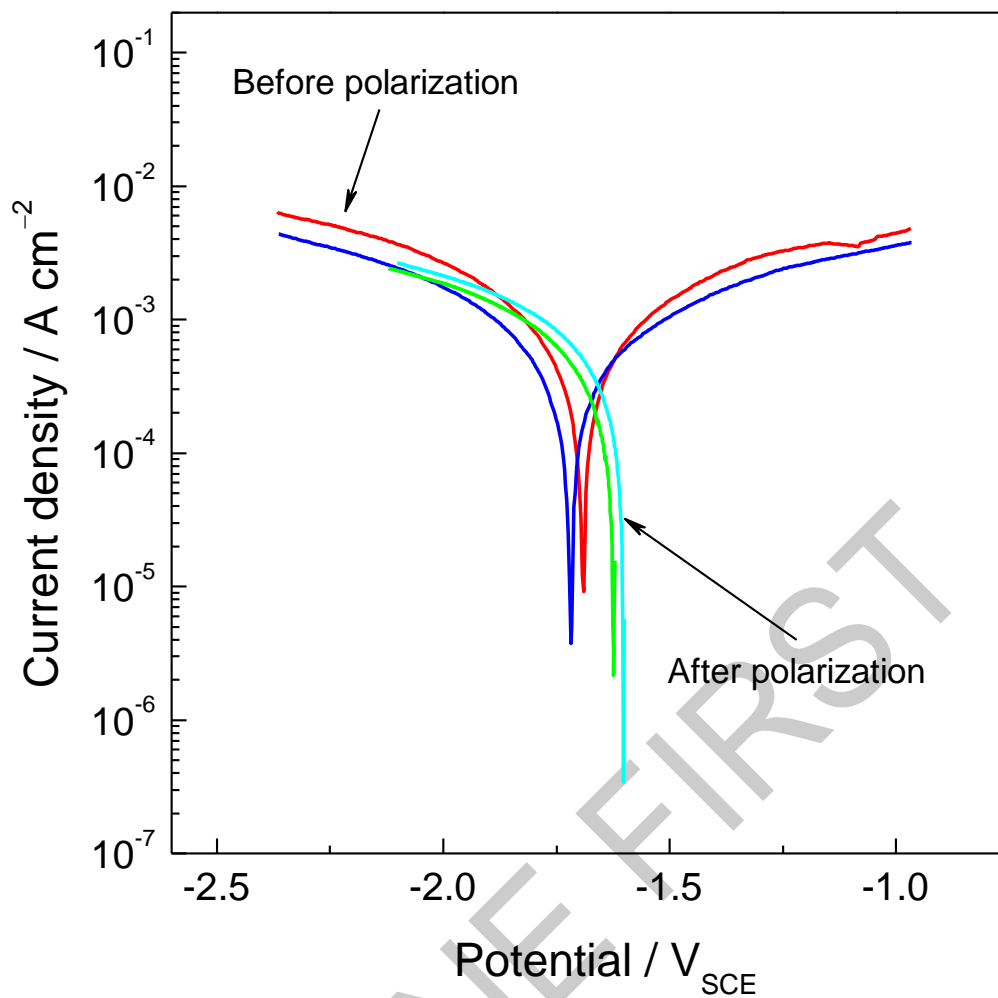


**Fig. 11.** Cathodic potentiodynamic polarization curves for HP Mg electrode in 0.1 M Citric Acid buffer (pH 3) solution after galvanodynamic anodic polarization up to +75 mA/cm<sup>2</sup>. Experiments were performed starting from the OCP at a potential scan rate of 1 mV/s. Data from duplicated experiments are presented. Current density is presented as absolute value.